Theor Chem Acc (2004) 112: 305–312
DOI 10.1007/s00214-004-0588-x

Theoretical Chemistry Accounts

Regular article

Theoretical study of the semihydrogenation of alkynes catalyzed by Pd(0) complexes: Is a zwitterionic pathway possible?

Alain Dedieu[1], **Stéphane Humbel**[2], **Cornelis J. Elsevier**[3], **Cedric Grauffel**[1]

[1] Laboratoire de Chimie Quantique, UMR 7551 CNRS/ULP, Université Louis Pasteur, 4 rue Blaise Pascal, 67000, Strasbourg, France
[2] UMR 6516 "Synthèse, Catalyse et Chiralité", ENSSPICAM-Faculté des Sciences Saint Jérôme, Avenue Escadrille Normandie-Niemen, 13397, Marseille Cedex 20, France
[3] Institute of Molecular Chemistry, Coordination and Organometallic Chemistry, University of Amsterdam, Nieuwe Achtergracht 166, 1018 WV, Amsterdam, The Netherlands

Received: 4 August 2003 / Accepted: 18 December 2003 / Published online: 10 August 2004

Abstract. Density functional theory B3LYP calculations have been carried out for the Pd(diimine)(C_2H_2) + H_2 → Pd(diimine)(C_2H_4) reaction, which is the key reaction in the semihydrogenation of alkynes homogeneously catalyzed by (diimine)palladium(0) complexes. The results show that a H_2 heterolytic addition across one Pd–N bond opens a feasible zwitterionic pathway for the catalytic process, and accounts for the pairwise transfer of the two hydrogen atoms inferred from parahydrogen induced polarization NMR experiments.

Keywords: H_2 heterolytic splitting – Density functional theory calculations – Homogeneous catalysis – Hydrogenation

Introduction

Conversion of alkynes into (*Z*)-alkenes is traditionally carried out via heterogeneous catalysis [1, 2, 3, 4, 5, 6, 7, 8, 9]. A few homogeneous catalyst systems based on palladium(0) complexes are also known [10, 11], among which a complex bearing the bidentate diimine ligand bis(arylimino)acenaphtene (hereafter abbreviated as bian)**1** [11].The mechanism postulated for the process is shown in Scheme 1: **1** should be considered as a pre-catalyst, and the actual catalyst is the [Pd(bian)alkyne] complex **2**. The catalytic cycle therefore comprises the reaction of **2** with hydrogen to yield the alkene complex **3**, and in **3** the substitution of the newly formed (*Z*)-alkene by the alkyne. Quite interestingly parahydrogen induced polarization (PHIP) NMR spectroscopy seems to be indicative of a pairwise transfer of the two hydrogen atoms [11]. Yet, the occurrence of such a pairwise transfer to the carbon–carbon bond via a homolytic splitting of H_2 is Woodward–Hoffmann-forbidden, at least suprafacially, since it is a $[\sigma_{2s} + \pi_{2s}]$ reaction. Moreover a concerted antarafacial approach is not likely on steric grounds. In order to elucidate this issue which is quite puzzling from a mechanistic point of view, we have undertaken a theoretical study of the whole homogeneous catalytic process. Various routes have been considered, the details of which will be reported elsewhere together with the experimental study. Here we rather wish to stress the feasibility of one specific route that had never been considered before and that involves, in a first step, a [2 + 2] *heterolytic* addition of H_2 across the Pd–N bond of **2**. We will also show that this step, which yields a zwitterionic $Pd(H)^-....HN^+$ intermediate is followed by a series of relatively easy insertion/elimination steps leading to the final palladium–alkene complex (vide infra).

Proceedings of the 11th International Congress of Quantum Chemistry satellite meeting in honour of Jean-Louis Rivail

This paper is dedicated Prof. Jean-Louis Rivail

Correspondence to: Alain Dedieu
e-mail: dedieu@quantix.u-strasbg.fr

Computational details

The calculations were carried out at the density functional theory B3LYP level [12, 13, 14] with the Gaussian 98 program [15] using as a model the [Pd(HN = CH–CH = NH)(C_2H_2)] system **4**. Some additional calculations were also carried out on the [Pd(bipyridine)(C_2H_2)] system, which is a model closer to **2**. The geometries were optimized by the gradient technique, using the standard LANL2DZ pseudo potential and basis sets for

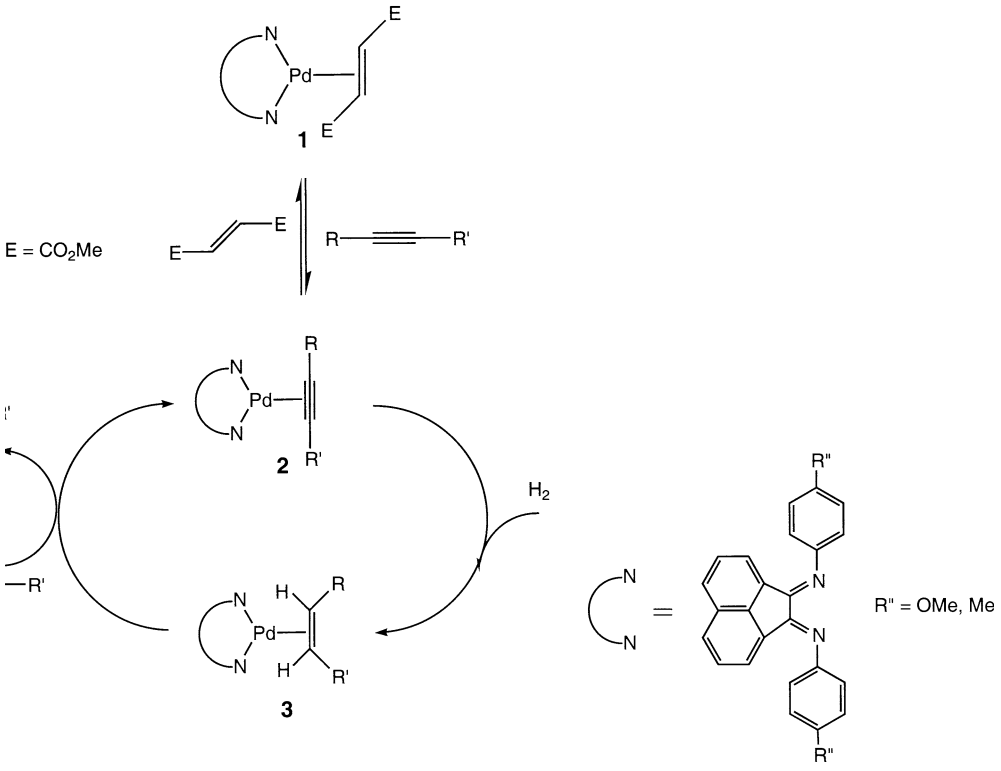

Scheme 1

all atoms [16, 17, 18]. The nature of the optimized structures, either transition states or intermediates, was assessed through a frequency calculation, and the changes of Gibbs free energies (ΔG values) were obtained by taking into account zero-point energies, thermal motion, and the entropy contribution at standard conditions (temperature of 298.15 K, pressure of 1 atm). The effect of a larger basis set (hereafter referred to as SDD*_6-311G**) was tested by carrying out single-point energy calculations at the LANL2DZ optimized geometries. In this SDD*_6-311G** basis set, the innermost core electrons of the palladium atom are described by the quasirelativistic energy-adjusted spin–orbit averaged effective core potential from the Stuttgart group and the remaining outer core and valence electrons by the associated triple-ζ basis set [19], to which an f-polarization function of exponent 1.472 [20] is added. The polarized triple-ζ 6-311G(d,p) basis set is used for C, N, and H [21]. Since the ΔE values obtained with both basis sets led to similar conclusions (vide infra), we

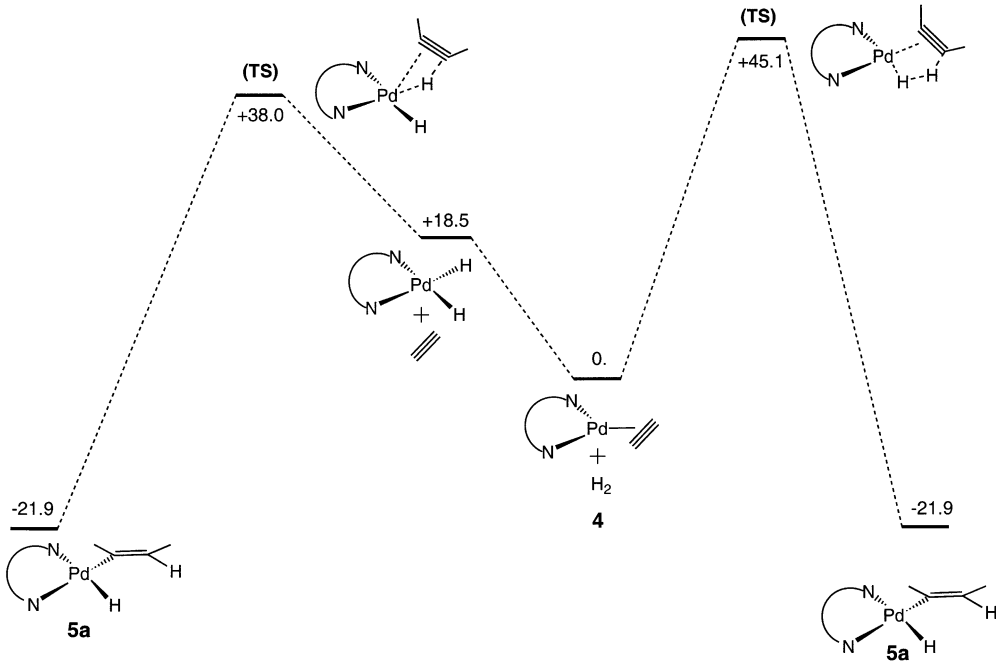

Fig. 1. Schematic energy profiles for the [2 + 2] addition of H_2 across the Pd–C bond of the [Pd(HN = CH–CH = NH)(C_2H_2)] palladium(0) complex (*right*) and for the acetylene insertion into the Pd–H bond of the [Pd$(H)_2$(HN = CH-CH = NH)(C_2H_2)] palladium(II) complex (*left*). The relative energies are in kilocalories per mole

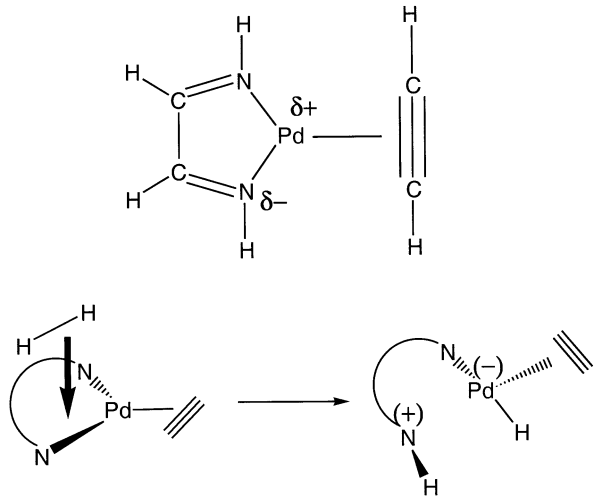

Scheme 2

concentrate our discussion on the LANL2DZ results for which enthalpy and free-energy values are available.

Results and discussion

Although their being forbidden we first looked for H_2 homolytic cleavage pathways that would account for the pairwise character of the H_2 transfer. Not unexpectedly, no transition state could be located for the $[\sigma_{2s}+\pi_{2s}]$ H_2 addition across the C–C triple bond of the C_2H_2 moiety, either in cyclopropene, which is the isolobal analog of $[Pd(HN=CH\text{-}CH=NH)(C_2H_2)]$, or in the $[Pd(HN=CH\text{-}CH=NH)(C_2H_2)]$ complex itself. In the latter case the search led instead to a transition state corresponding to an addition across the Pd–C bond, the details of which will be reported elsewhere. Here we have sketched on the right side of Fig. 1 the course of this addition, which yields the vinyl–hydrido–palladium complex **5a**. Note that this addition is also a [2+2] Woodward–Hoffmann-forbidden reaction. The corresponding energy barrier is therefore very high ($\Delta E^{\ddagger} = +45.1$ kcal mol^{-1}), despite an exothermicity of -21.5 kcal mol^{-1} between **4** and **5a**.

Rather than considering, as previously, the reaction of dihydrogen with a Pd(0)–alkyne complex, one could instead consider the reaction of a Pd(II)–dihydride with the alkyne. A pathway involving the transfer of the two hydrogen atoms from the dihydrido $[Pd(H)_2(HN=CH\text{-}CH=NH)]$ complex to free C_2H_2 was therefore searched. In contrast to the $[2s+2s]$ reactions, such a transfer would be a $[\sigma_{4s}+\pi_{2s}]$ reaction, analogous to the transfer of two hydrogens from ethane to acetylene to give two ethylene molecules, and hence should be allowed. Yet the transition-state optimization procedure led, as drawn schematically on the left side of Fig. 1, to a geometry indicative of an acetylene insertion into the Pd–H bond, the product of this insertion being again the vinyl–hydrido–palladium complex **5a**. The corresponding energy barrier from $[Pd(H)_2(HN=CH\text{-}CH=NH)]+C_2H_2$ is relatively moderate, 19.5 kcal mol^{-1}. One has, however, to add to this value the endothermicity of the oxidative addition reaction $[Pd(HN=CH\text{-}CH=NH)(C_2H_2)]+H_2 \rightarrow [Pd(H)_2(HN=CH\text{-}CH=NH)]+C_2H_2$. That the oxidative addition of H_2 to Pd(0) complexes is an endothermic reaction is a feature that is well documented, both experimentally and theoretically [22, 23, 24, 25]. For the $[Pd(HN=CH\text{-}CH=NH)(C_2H_2)]$ system this endothermicity amounts to $+18.5$ kcal mol^{-1}. The net result is a high energy barrier to reach the transition state from $[Pd(HN=CH\text{-}CH=NH)(C_2H_2)]+H_2$, 38.0 kcal mol^{-1} (Fig. 1, left).

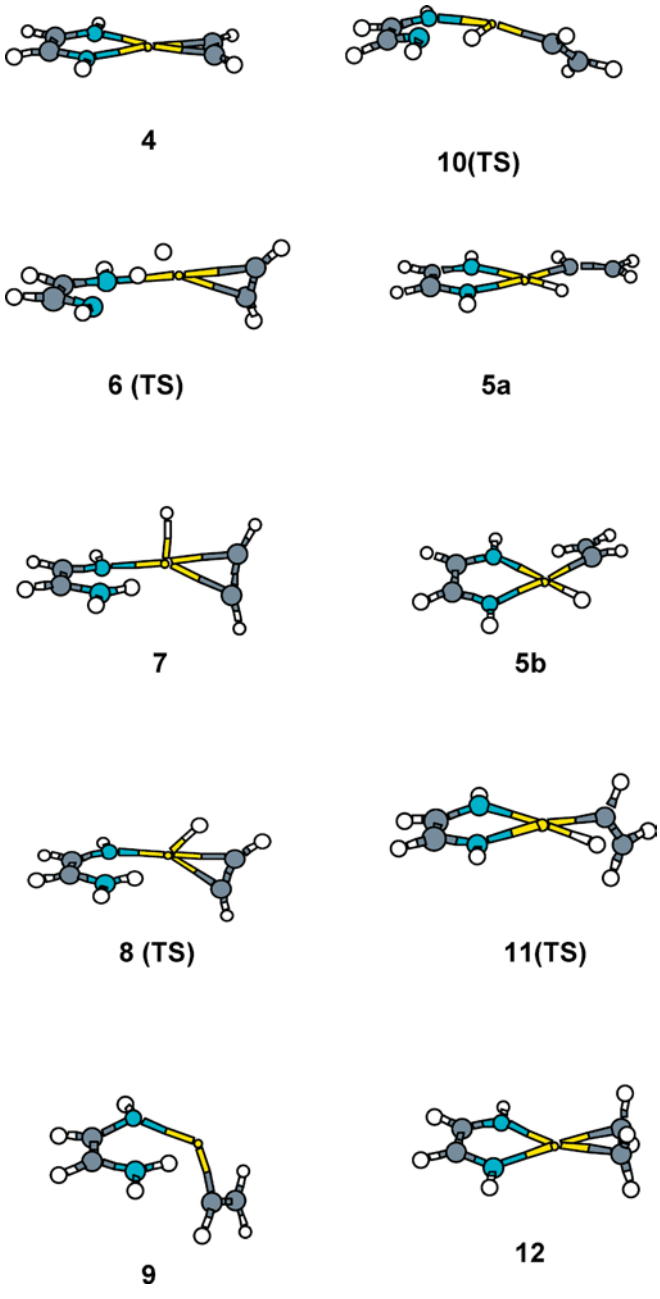

Fig. 2. Optimized structures of systems **4**–**11**

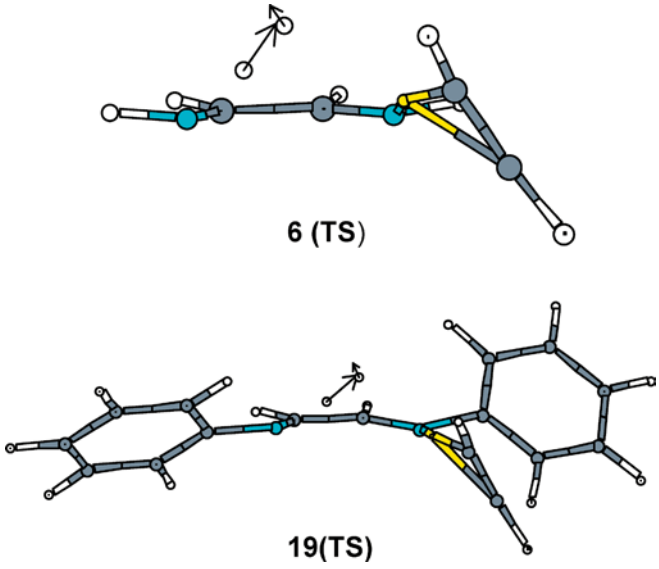

Fig. 3. Optimized structure and imaginary mode of the transition states for the H_2 heterolytic splitting reaction with [Pd(HN=CH-CH=NH)(C_2H_2)], ***6** (TS)*, and [Pd(bipyridine)(C_2H_2)], ***19** (TS)*

It is therefore clear that the pathways that would combine a homolytic cleavage of H_2 and the pairwise character of the transfer of the hydrogen atoms are quite energy demanding. Keeping the pairwise transfer character inferred from the PHIP NMR experiments, we were therefore led to consider as a first step of the catalytic cycle the heterolytic splitting of H_2 (Scheme 2). Although not common, the heterolytic splitting of H_2 across a late transition metal-to-ligand σ bond has been put forth in several instances [24, 26, 27, 28, 29, 30, 31, 32]. We have previously stressed that it is favored by the presence on the ligand of a lone pair which is not engaged in the σ bond and, more critically, by the polarity of the metal-to-ligand bond [27, 28, 33]. In our case the diimine ligand has π occupied orbitals that involve the nitrogen atoms and that are perpendicular to the plane of the diimine. In addition the Pd–diimine bond is quite polar: the charges on palladium and on nitrogen are +0.210e and −0.395e respectively (Mulliken charges). The charge separation obtained from the natural bond orbital analysis is greater, as generally observed [34, 35], +0.513e for palladium and −0.712e for nitrogen. As a result of this rather large charge separation one finds a relatively low energy transition state, **6**, lying +21.5 kcal mol^{-1} above the [Pd(HN=CH–CH=NH)(C_2H_2)]+H_2 reactants, and leading to the $\{[Pd(C_2H_2)(H)]^-(NH=CH–CH=NH_2)^+\}$ complex **7**. The structure of **6** is shown in Fig. 2. The single imaginary mode is displayed in Fig. 3, the corresponding imaginary frequency being 1,005*i* cm^{-1}. In **6** the H–H bond has elongated from 0.744 Å in free H_2 to 0.935 Å. The N...H and Pd...H distances amount to 1.399 and 1.825 Å, respectively. The N..H..H moiety is almost linear, the corresponding angle being 170.5°. On the other hand the Pd..H..H unit differs markedly from linearity, the angle being 98.2°. These values correspond to the nature of the bonding in the N..H..H..Pd unit, viz., a nascent proton interacting with two negatively charged atoms (the nitrogen atom and the hydrogen atom migrating towards the palladium atom), and a nascent hydride interacting with two positively charged atoms (the palladium atom and the hydrogen atom migrating towards the nitrogen atom). One can also view the N..H..H..Pd unit as involving a dihydrogen bond [36, 37, 38]. We have in the past encountered a somewhat similar transition state for the H_2 elimination from a zwitterionic Pd(IV) complex [39]. The computed energy barrier between **6** and [**4**+H_2] amounts to 21.5 kcal mol^{-1}. Including the zero-point vibrational energy and the thermal corrections leads to a similar value for the enthalpy barrier, 21.3 kcal mol^{-1}. The corresponding free-energy value is of course somewhat greater, 29.3 kcal mol^{-1}, owing to the positive entropy term.

The heterolytic splitting of H_2 therefore opens a pathway that can be divided into two parts, summarized in Fig. 4. The first part (Fig. 4a) involves intermediates and transition states, the nature of which is essentially zwitterionic. It ends with the neutral vinyl–hydrido intermediate **5a**. In the second part of the pathway (Fig. 4b) a vinyl insertion into the palladium hydride bond of **5a** takes place. It leads, via transition state **11**, to the palladium–ethylene complex **12**.

The optimized geometries of the reactants, transition states and intermediates of both parts (**4**–**12**) are shown in Fig. 2, the corresponding energies are collected in Table 1 and the most important geometrical parameters in Table 2.

The structure of intermediate **7** obtained immediately after the heterolytic splitting of H_2 is well representative of the zwitterionic nature of the system, i.e., $\{[Pd(C_2H_2)(H)]^-(NH=CH–CH=NH_2)^+\}$: the geometry around the dissociated nitrogen atom is essentially planar (the C–N–H–H dihedral angle is 5°). There is probably weak interaction between the proton on the nitrogen and the palladium atom, exemplified by the Pd...$H_{(N)}$ distance of 2.36 Å. The Mulliken charges of the NH_2 and PdH unit are +0.088e and −0.135e, respectively. **7** is somewhat higher in energy than the reactants [Pd(HN=CH-CH=NH)(C_2H_2)]+H_2, see Table 1. The ΔH value is 5.4 kcal mol^{-1}, the ΔG value is, as for transition state **6**, larger, viz., 12.2 kcal mol^{-1}, owing to the positive entropy term.

The steps that follow the H_2 heterolytic splitting correspond to the sequential transfer of the two hydrogen atoms to the coordinated acetylene. The hydride is transferred first, via transition state **8**. This leads to the zwitterionic vinyl species $\{[Pd(C_2H_3)]^-(NH=CH–CH=NH_2)^+\}$ **9**, see Fig. 4a. The barrier for this transfer is low, 5.6 kcal mol^{-1}. The corresponding $\Delta H^{\ddagger}$ and $\Delta G^{\ddagger}$ are similar (Table 1), owing to the absence in this step, which is intramolecular, of marked entropy effects. The zwitterionic vinyl species $\{[Pd(C_2H_3)]^-(NH=CH–CH=NH_2)^+\}$ **9** is the lowest point on the energy profile

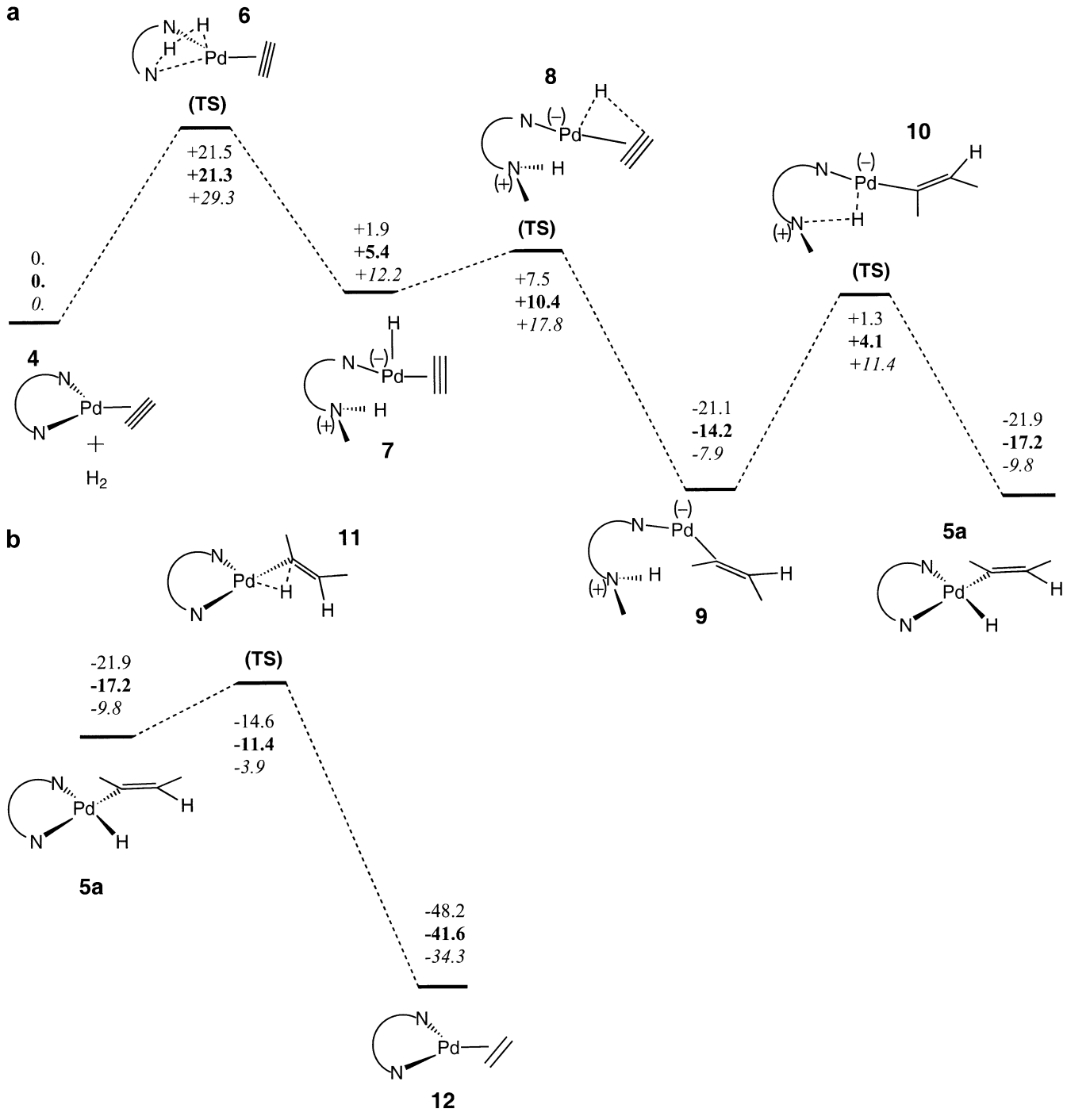

Fig. 4. Schematic energy profiles for **a** the first part and **b** the second part of the zwitterrionic pathway in the semihydrogenation of C_2H_2 catalyzed by [Pd(HN=CH–CH=NH)(C_2H_2)]. The relative energies are in kilocalories per mole. ΔH values are in *bold*, and ΔG values in *italics*. The zero of energy corresponds to [Pd(HN=CH–CH=NH)(C_2H_2)] + H_2

of Fig. 4a. As in **7** there may be some weak interaction between the proton on the nitrogen and the palladium atom, the Pd...$H_{(N)}$ distance (2.41 Å) being similar to the one in **7**. The proton transfer from the nitrogen atom to the palladium atom comes next. This is in fact an oxidative addition which has an energy barrier comparable to the H_2 heterolytic splitting reaction: the $\Delta E^{\ddagger}$ value between **9** and transition state **10** amounts to 22.4 kcal mol^{-1}, but the $\Delta H^{\ddagger}$ and $\Delta G^{\ddagger}$ values are smaller, especially the $\Delta G^{\ddagger}$ value, 18.3 and 19.3 kcal mol^{-1}, instead of 21.3 and 29.3 kcal mol^{-1} for the H_2 heterolytic splitting step. The structure of **5a**, the vinyl–hydrido intermediate which is the product of this proton transfer step, was obtained by relaxing the geometry of **10**. Note that in **5a** the hydride is trans to the hydrogen of the CH unit of the vinyl ligand.

Table 1. Relative energies (ΔE), enthalpies (ΔH) and free energies (ΔG) for the reactants, intermediates, transition states and products. The values are in kilocalories per mole. The B3LYP/LANL2DZ total energies of $[Pd(HN=CH–CH=NH)(C_2H_2)]+H_2$ (in atomic units) are $E=-393.34470$, $H=-393.22733$ and $G=-393.28437$. The ΔE values in parentheses refer to the B3LYP/SDD*_6-311G**//B3LYP/LANL2DZ single-point calculations. The E value for $[Pd(HN=CH–CH=NH)(C_2H_2)]+H_2$ is −394.65606 au

System	ΔE	ΔH	ΔG
$[Pd(HN=CH–CH=NH)(C_2H_2)]$(**4**) + H_2	0	0	0
6 (TS)	+21.5(+21.2)	+21.3	+29.3
$\{[Pd(C_2H_2)(H)]^-(NH=CH–CH=NH_2)^+\}$ (**7**)	+1.9(+5.5)	+5.4	+12.2
8 (TS)	+7.5(+10.2)	+10.4	+17.8
$\{[Pd(C_2H_3)]^-(NH=CH–CH=NH_2)^+\}$ (**9**)	−21.1 (−10.7)	−14.2	−7.9
10 (TS)	+1.3(+3.8)	+4.1	+11.4
$[Pd(HN=CH–CH=NH)(H)(C_2H_3)]$(**5a**)	−21.9 (−18.9)	−17.2	−9.8
$[Pd(HN=CH–CH=NH)(H)(C_2H_3)]$(**5b**)	−22.6 (−19.4)	−17.9	−9.8
11 (TS)	−14.6 (−12.3)	−11.4	−3.9
$[Pd(HN=CH–CH=NH)(C_2H_4)]$(**12**)	−48.2 (−44.0)	−41.6	−34.3
$[Pd(bipy)(C_2H_2)]$(**13**) + H_2	0	0	0
19 (TS)	+24.8	+24.4	+31.7
$\{[Pd(C_2H_2)(H)]^-(bipyH)^+\}$**20**	+7.8	+11.3	+17.6

Table 2. Some optimized bond distances (in angstroms) for the reactants, intermediates, transition states and products

System	Pd–C_α[a]	Pd–C_β	Pd–N_β[b]	H–N_β	Pd–H	H–C_β	H..H
$[Pd(HN=CH-CH=NH)(C_2H_2)]$(**4**) + H_2	2.047	2.047	2.148	–	–	–	0.744
6 (TS)	2.152	2.113	3.199	1.399	1.825	2.966	0.935
$\{[Pd(C_2H_2)(H)]^-(NH=CH–CH=NH_2)^+\}$ (**7**)	2.210	2.178	3.216	1.018	1.580	2.454	2.791
8 (TS)	2.128	2.176	3.224	1.018	1.620	1.697	3.042
$\{[Pd(C_2H_3)]^-(NH=CH–CH=NH_2)^+\}$ (**9**)	1.992	2.959	3.250	1.020	3.130	1.090	–
10 (TS)	2.006	2.982	3.088	1.741	1.561	1.091	–
$[Pd(HN=CH–CH=NH)(H)(C_2H_3)]$(**5a**)	1.997	3.079	2.113	2.834	1.563	1.087	–
$[Pd(HN=CH–CH=NH)(H)(C_2H_3)]$(**5b**)	2.005	2.964	2.117	2.844	1.568	1.092	–
11 (TS)	2.045	3.092	2.162	3.327	1.622	1.088	–
$[Pd(HN=CH–CH=NH)(C_2H_4)]$(**12**)	2.138	2.138	2.193	–	–	1.090	–
$[Pd(bipy)(C_2H_2)]$(**13**) + H_2	2.056	2.056	2.191	–	–	–	0.744
19 (TS)	2.161	2.113	3.149	1.391	1.810	2.931	0.954
$\{[Pd(C_2H_2)(H)]^-(bipyH)^+\}$**20**	2.225	2.187	3.148	1.024	1.577	2.459	2.708

[a]Carbon atom that remains bound to Pd throughout the reaction
[b]Nitrogen atom that is dissociated from Pd upon H_2 addition

A slightly more stable isomer, **5b**, was optimized independently. **5b** is more stable than **5a** by only 0.7 kcal mol^{-1}, see Table 1. It corresponds to a rotation of the vinyl unit around the Pd–vinyl bond. The vinyl ligand should therefore rotate almost freely. In fact the transition state for the last step of this route, viz., the vinyl insertion into the Pd–hydride bond (Fig. 4b), has a geometry in which the vinyl group is perpendicular to the coordination plane, see **11**: the C–C–Pd–H dihedral angle amounts to 92.6°. This vinyl insertion leads to the palladium–ethylene complex **6**. It is an easy process: the reaction energy **5a** → **12** amounts to −26.3 kcal mol^{-1} and the energy barrier between **6** and **11** is only +7.3 kcal mol^{-1}. The corresponding $\Delta H^{\ddagger}$, ΔH, $\Delta G^{\ddagger}$ and ΔG of this intramolecular step are again quite similar (Table 1).

An analogous energy profile is obtained from the single-point SDD*_6-311G** calculations. As seen from Table 1 the SDD*_6-311G**//LANL2DZ ΔE values and the LANL2DZ//LANL2DZ values are quite similar. In particular, the SDD*_6-311G** computed reaction energy for the heterolytic H_2 addition step amounts to +5.4 kcal mol^{-1}, the energy barrier being 21.2 kcal mol^{-1}. The corresponding LANL2DZ//LANL2DZ values are +1.9 and 21.5 kcal mol^{-1}. The largest difference is found for the zwitterionic vinyl species $\{[Pd(C_2H_3)]^-(NH=CH–CH=NH_2)^+\}$ **9**, which is below $[Pd(HN=CH–CH=NH)(C_2H_2)]+H_2$ by only 10.7 kcal mol^{-1}. As a result the energy barrier for the subsequent proton migration from the nitrogen atom is now definitively smaller than the barrier for the H_2 heterolytic splitting. This confirms the rate-determining nature of the H_2 heterolytic splitting step.

One may, of course, also worry about the ability of the $[Pd(HN=CH–CH=NH)(C_2H_2)]$ system to model the real $[Pd(bian)(C_2R_2)]$ complexes of Scheme 1, especially if one bears in mind the influence of the polarity of the Pd–N bond on the ease of the H_2 heterolytic splitting. In order to assess this point we carried out additional calculations on the $[Pd(diimine)(C_2H_2)]$ systems **13**–**18**, in which the diimine ligand is either bipyridine (**13**), substituted bipyridines (**14**, **15**), bis(imino)acenaphtene (**16**), bis(phenylimino)acenaphtene (**17**), or bis(tolylimino)acenaphtene (**18**), see Fig. 5. The geometries of these systems were optimized at the density functional theory B3LYP/LANL2DZ level,

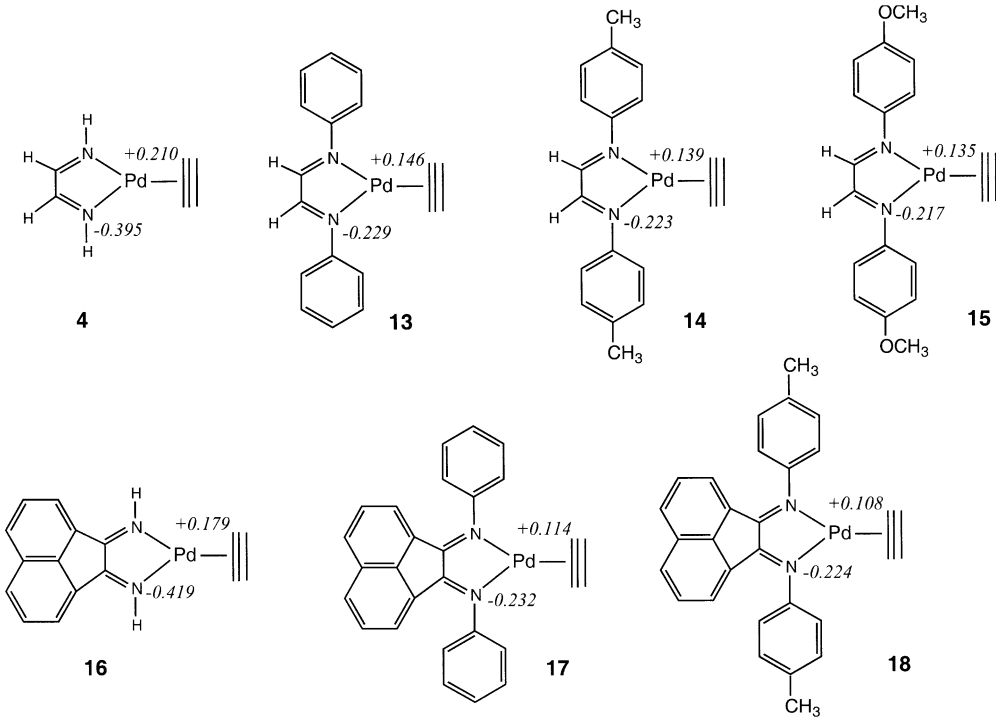

Fig. 5. Mulliken charges of the palladium and nitrogen atoms for various diimine ligands of the (diimine)Pd(0)acetylene complex

retaining the C_2 symmetry. The results of the Mulliken population analysis for the Pd–N bond are also shown in Fig. 5. They first indicate that the polarity of the Pd–N bond is relatively insensitive to the para substitution of the phenyl groups. They also indicate that the [Pd(bipyridine)(C_2H_2)] model system (**13**) is rather close to the experimental [Pd(bis(tolylimino)acenaphtene)(C_2H_2)] system (**18**). Compared with **4**, the polarity of the Pd–N bond in **13** or in **18** is somewhat decreased, but one may reasonably expect that the charge separation (e.g., +0.146e on Pd and −0.229 on N for **13**) is large enough that a relatively low energy barrier for the H_2 heterolytic splitting across this bond will remain. Indeed the determination of transition state **19** for the reaction of H_2 with **13** led to an energy barrier which is still moderate: the ΔE value amounts to 24.8 kcal mol^{-1}, see Table 1. The geometries of **19** and **6** are also very similar (Fig. 3, Table 2), as are the respective imaginary frequencies (1,005*i* and 1,101*i* cm^{-1}). At this stage it also is worth pointing out that solvation effects should favor the zwitterionic pathway: previous theoretical studies that we carried out on a [$Pd(II)^{-}$...NH^{+}]/Pd(IV) pair of isomers indicated a preference for the zwitterionic isomer upon solvation in dichloromethane [40, 41].

Thus, in conclusion, all our results point to the feasibility of a zwitterionic route for the semihydrogenation of alkynes homogeneously catalyzed by diimine Pd(0) complexes. They also agree with the experimental results, since the H_2 heterolytic splitting, which implies a pairwise transfer of the hydrogen atoms, appears to be the rate-determining step in this route.

Acknowledgements. The calculations were carried out on the workstations of our laboratory and of the Centre Universitaire Régional de Ressources Informatiques of Strasbourg. We thank D.L. Padel and S. Fersing for their help and technical assistance. S.H. gratefully acknowledges the CNRS for the financing of one sabbatical year and the UMR6519 of the Université de Reims for financial support during his stay in Strasbourg.

References

1. Lindlar H (1952) Helv Chim Acta 35:446
2. Lindlar H, Dubuis R (1966) Org Synth 46:89
3. McEwenAB, Guttieri MJ, Maier WF, Laine RM, Shvo Y (1983) J Org Chem 48:4436
4. Ulan JG, Maier WF, Smith DA (1987) J Org Chem 52:3132
5. Choudary BM, Vasantha G, Sharma M, Barathi P (1989) Angew Chem Int Ed Engl 28:465
6. Sulman E, Matveeva V, Usanov A, Kosivtsov Y, Demidenko G, Bronstein L, Chernyshov D, Valetsky P (1999) J Mol Catal 146:265
7. Gruttadauria M, Noto R, Deganello G, Liotta LF (1999) Tetrahedron Lett 40:2857
8. Gruttadauria M, Liotta LF, Noto R, Deganello G (2001) Tetrahedron Lett 42:2015
9. Spee MPR, Boersma J, Meijer MD, Slagt MQ, van Koten G, Geus JW (2001) J Org Chem 66:1647
10. Stern EW, Maples PK (1972) J Catal 27:120
11. van Laren MW, Elsevier CJ (1999) Angew Chem Int Ed Engl 38:3715
12. Becke AD (1988) Phys Rev A 38:3098
13. Lee C, Yang W, Parr RG (1988) Phys Rev B 37:785
14. Becke AD (1993) J Chem Phys 98:5648
15. Frisch MJ, Trucks GW, Schlegel HB, Scuseria GE, Robb MA, Cheeseman JR, Zakrewski VG, Montgomery JA Jr, Statmann RE, Burant JC, Dapprich S, Millam JM, Daniels AD, Kudin KN, Strain MC, Farkas O, Tomasi J, Barone V, Cossi M, Cammi R, Mennucci B, Pomelli C, Adamo C, Clifford S, Ochterski J, Petersson GA, Ayala PY, Cui Q, Morokuma K, Malick DK, Rabuck AD, Raghavachari K, Foresman JB,

Ciolowski J, Ortiz JV, Stafanov BB, Liu G, Liashenko A, Piskorkz P, Komaroni I, Gomperts R, Martin RL, Fox DJ, Keith T, Al-Laham MA, Peng CY, Nanayakkara A, Gonzales C, Challacobe M, Gill PMW, Johnson B, Chen W, Wong MW, Andres JL, Head-Gordon M, Reploge ES, Pople JA (1998) Gaussian98, revision A.5. Gaussian, Pittsburgh, PA
16. Hay PJ (1985) J Chem Phys 82:299
17. Dunning TH, Hay PJ (1976) Modern theoretical chemistry. Plenum, New York, p 1
18. Huzinaga S (1965) J Chem Phys 42:1293
19. Andrae D, Haüssermann U, Dolg M, Stoll H, Preuss H (1990) Theor Chim Acta 77:123
20. Ehlers AW, Böhme M, Dapprich S, Gobbi A, Höllwarth JV, Köhler KF, Stegmann R, Veldkamp A, Frenking G (1993) Chem Phys Lett 208:237
21. Krishnan R, Binkley JS, Seeger R, Pople JA (1980) J Chem Phys 72:650
22. Yoshida T, Otsuka S (1977) J Am Chem Soc 99:2134
23. Low JJ, Goddard WA III (1986) Organometallics 5:610
24. Niu S, Hall MB (2000) Chem Rev 100:353
25. Dedieu A (2000) Chem Rev 100:543
26. Hutschka F, Dedieu A, Leitner W (1995) Angew Chem Int Ed Engl 34:1742
27. Hutschka F, Dedieu A, Eichberger M, Fornika R, Leitner W (1997) J Am Chem Soc 119:4432
28. Milet A, Dedieu A, Kapteijn G, van Koten G (1997) Inorg Chem 36:3223
29. Musaev DG, Froese RDJ, Morokuma K (1997) New J Chem 21:1269
30. Musaev DG, Svensson M, Morokuma K, Strömberg S, Zetterberg K, Siegbahn PEM (1997) Organometallics 16:1933
31. Musaev DG, Froese RDJ, Morokuma K (1998) Organometallics 17:1850
32. Musashi Y, Sakaki S (2002) J Am Chem Soc 124:7588
33. Dedieu A, Hutschka F, Milet A (1999) In: Truhlar DG, Morokuma K (eds) ACS symposium series 721. American Chemical Society, Washington, DC, p 100
34. Wiberg KW, Rablen PR (1993) J Comput Chem 14:1504
35. Cramer CJ (2002) Essentials of computational chemistry. Wiley, Chichester, p 278
36. Crabtree RH, Siegbahn PEM, Eisenstein O, Rheingold AL, Koetzle TF (1996) Acc Chem Res 29:348
37. Custelcean R, Jackson JE (2001) Chem Rev 101:1963
38. Alkorta I, Elguero J, Mo O, Yanez M, Del Bene JE (2002) J Phys Chem A 106:9325
39. Milet A, Dedieu A, Canty AJ (1997) Organometallics 16:5331
40. Visentin T, Kochanski E, Moszynski R, Dedieu A (2001) J Phys Chem A 105:2023
41. Visentin T, Kochanski E, Moszynski R, Dedieu A (2001) J Phys Chem A 105:2031